ELSEVIER

Journal of Nuclear Materials 290–293 (2001) 326–330

journal of nuclear materials

www.elsevier.nl/locate/jnucmat

Studies of tungsten erosion at the inner and outer main chamber wall of the ASDEX Upgrade tokamak

A. Tabasso *, H. Maier, J. Roth, K. Krieger, ASDEX Upgrade Team

Max-Planck-Institut für Plasmaphysik, EURATOM Association, Boltzmannstraße 2, D-85748 Garching bei München, Germany

Abstract

A critical issue for the choice of main chamber first wall materials in future fusion devices such as ITER is the erosion rate due to bombardment by charge-exchange (CX) neutrals. Due to the relatively small flux density of impacting particles, respective measurements are only possible using long term samples (LTS) exposed for a full experimental campaign. In ASDEX Upgrade, CX erosion has been studied extensively for tungsten on the inner heat shield by placing four W coated tiles at different poloidal positions in one toroidal sector. During the same campaign, several LTS were placed at different poloidal and toroidal positions of the outer wall. ^{13}C and Cu coated graphite probes were also used in order to test and compare W low and medium Z alternatives. The erosion results from the probes are compared with the calculated erosion [W. Eckstein, C. Garcia-Rosales, J. Roth, W. Ottenberger IPP Report, IPP 9/82]; [H. Verbeek, J. Stober, D. Coster, W. Eckstein, R. Schneider Nucl. Fus. 38 (1998) 12] and a figure of merit (F. of M.) between several materials is proposed which also takes into account the plasma isotope effect in CX erosion.

Keywords: Erosion; Tokamak; Charge exchange

1. Introduction

Tungsten is being considered as one of the candidate materials for plasma facing components of future fusion devices [3]. Apart from its high energy threshold for sputtering, W does not suffer from chemical sputtering as for example carbon. Furthermore, tritium does not co-deposit with W [4], which poses a serious material activation problem as in the case of carbon. It is, however, important to keep W erosion under strict control. W is a high Z material and even concentrations in the range of 2×10^{-5} in the plasma would be sufficient to prevent ignition from taking place, because of radiation cooling in the core [5]. It is therefore of prime importance in view of a next step device, such as ITER, to investigate the feasibility of using W both as divertor and as a first wall material.

2. Experimental set-up and method

W coated graphite tiles were installed in sector 6 at four different poloidal positions on the inner heat shield [6] and exposed for a full experimental campaign. The tiles were analysed before and after exposure by Rutherford backscattering (RBS) and proton induced X-ray emission (PIXE) techniques. The analysis spots were 1 mm^2 in size, equally spaced and located 5 mm from the right, left, top and bottom edges of the tiles. Details of the experimental set-up, analysis techniques and error bars of the measurement can be found in [6]. To study the toroidal and poloidal variation of erosion on the outer wall, one toroidal and one poloidal set of long term samples (LTS) were employed during the same and successive campaigns. Graphite samples were covered with thin W, ^{13}C and Cu layers by vapour deposition. Almost every tokamak sector had a LTS at mid-plane and sector 5 had six LTS poloidally arranged around the vacuum vessel. See [7] for the poloidal distribution of the LTS and for a drawing of the magnetically operated shutters which protected the probes from B and Si

* Corresponding author. Tel.: +49-89 3299 1495; fax: +49-89 3299 1149.

E-mail address: alberto.tabasso@ipp.mpg.de (A. Tabasso).

0022-3115/01/$ - see front matter
PII: S0022-3115(00)00437-2

depositions caused by the boronisation and siliconisation of the wall. During the first campaign (the same as for W coated tiles), W and ^{13}C coated were exposed, while in the second campaign W and Cu coated probes were inserted in the tokamak. Also in the probes case, the original and residual coating thickness were measured with RBS and PIXE analysis. The first campaign (December 1998–August 1999) consisted of 710 successful discharges for a total plasma exposure of ~4235 s (see [6] for a discharge statistic), while the second campaign (November 1999–February 2000) had 234 plasma pulses for a total discharge time of ~1515 s.

3. Experimental and modelling results

Figs. 1(a) and (b) show the poloidal distribution of W erosion on the right and left side (upstream and downstream plasma side, respectively) of the four heat shield tiles. In the figures, the erosion estimated for charge-exchange (CX) neutrals sputtering is also plotted. This latter result is calculated on the basis of B2/EIRENE modelling of the CX particle flux checked against the measurements of both a low energy particle analyser (LENA) and spectroscopic measurements of the hydrogen recycling flux, as measured in a previous experimental campaign for the divertor phase only [2]. The CX flux spectrum was calculated in [2] for a hydrogen plasma discharge. However, most of the discharges of the experimental campaign in question were fuelled with deuterium. The CX flux was, therefore, scaled taking into account the influence of the isotope change on the energy distribution of the neutral particles [8]. The calculated flux, for the shield position where it was at its maximum, was folded with the W physical sputtering coefficient for the appropriate projectile isotope [1] and integrated over energy. The result was finally multiplied by the total discharge time of the respective experimental campaign. From the two figures it is, however, clear that while the four tiles results for the right side and the upper tile (position 4) for the left one are in good agreement with the calculation, the left side results of the other three tiles are not. The left side measurement of tiles 8, 11 and 13, positioned in the lower half of the shield show clear evidence that in addition to CX sputtering, additional erosion mechanisms must be invoked in order to account for the amount of measured erosion. These show an erosion that is around a factor of three larger than calculated and measured in the right side of all tiles and in the left side of tile 4. The small poloidal asymmetries of the erosion profiles can be attributed to slight misalignment of the tiles and local flux variations. In Fig. 2, the toroidal erosion profiles in the top edge of the three lower tiles (8, 11, and 13) show very pronounced toroidal asymmetries. In contrast, the upper tile (position 4) has been eroded uniformly. Again, the erosion of W, as expected for only CX neutral sputtering, is plotted in the graph. Once more for the three lower tiles, the erosion is a factor of ~3 higher on the left side of the tiles than on the right side. The bottom edge erosion profiles show virtually identical results [6]. The asymmetric toroidal erosion is clear evidence for sputtering by ion impact being the dominant erosion mechanism. The observed lower erosion in the most right-hand edge of the tiles results from the shadowing effect of the upstream neighbouring tile. This is due to the fact that the flat tiles are arranged as a polygon within a cylindrical surface and that the magnetic field lines intersect the target at a very shallow angle of incidence. If the erosion was dominated by neutrals, this effect would not occur, as the neutral particles do not follow the magnetic field lines. The ion erosion is however not observed on tile 4. By looking at the magnetic configuration and at the plasma parameters (from

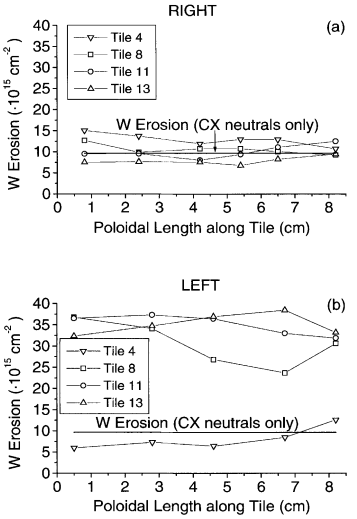

Fig. 1. Poloidal profiles of tungsten erosion for the right (a) and left (b) side of the four W coated tiles. In the graph, the expected erosion from sputtering by CX neutrals is plotted for comparison.

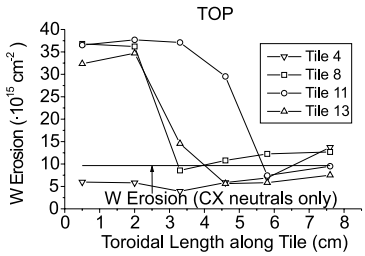

Fig. 2. Toroidal profiles of tungsten erosion on the top of the four W coated tiles. In the graph, the expected erosion from sputtering by CX neutrals is plotted for comparison.

EIRENE simulations [9]) during the flat top phase of divertor discharges, one sees no difference in the distance wall-separatrix or in the values of T_i or n_i, between the position of tile 4 and the position of tile 11 or 13. Furthermore, the typical distance wall-separatrix of ~10 cm guarantees the density and temperature of incident ions to be low enough not to produce any significant sputtering. This may hint to the fact that most of the ion erosion is caused by the internal transport barrier discharges (ITB) where the plasma is additionally heated during the limiter phase. This is however most probably not correct; in fact, during the NB heated limiter phase of these discharges, the plasma-separatrix is equally distant from tile 4 and 13. Hence, if those discharges were the cause of erosion, tile 4 should also see ion erosion. The only possible explanation is, therefore, that this additional ion erosion comes from the starting phase of all discharges. In ASDEX Upgrade, in fact, all plasmas are first formed on the lower heat shield, grown and moved higher up in a limiter phase until, finally, the divertor is formed. In this phase, the plasma has a quite low density (ranging from 5×10^{18} to 1×10^{19} m^{-3}) and it is, therefore, hot enough to justify a certain degree of sputtering. It is, however, important, as far as future devices are concerned, to be able to exclude ion erosion during the divertor phase of the discharges. In a possible future device, the plasma can, in fact, be formed on a specially suited limiter not built from W.

Figs. 3 and 4 show the toroidal erosion profiles (at the outer mid-plane) of W and ^{13}C probes exposed in the same campaign in which the W tiles were used. As can be seen in the case of W, the agreement between calculated and measured erosion is quite good. It has to be noticed that the probe in toroidal sector 5 had a malfunctioning shutter, which remained partially closed preventing the W probe from being exposed. In the case of the ^{13}C probes, the measured erosion, which is ~300 times higher than in the W case, is compared with the calculated ones using physical sputtering only and both

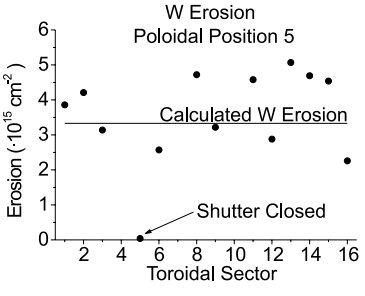

Fig. 3. Toroidal distribution of W erosion during the same experimental campaign in which the W coated tiles were exposed (December 1998–August 1999). In the graph, the expected erosion from sputtering by CX neutrals is plotted for comparison.

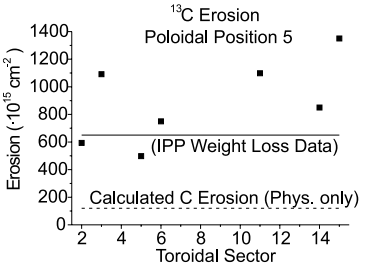

Fig. 4. Toroidal distribution of ^{13}C erosion during the same experimental campaign in which the W coated tiles were exposed (December 1998–August 1999). In the graph, the expected erosion from sputtering by CX neutrals is plotted for comparison. The dashed line represents erosion by physical sputtering only, the solid line by both physical and chemical sputtering. The chemical sputtering calculation is based upon IPP weight loss measurement data [10,11].

physical and chemical sputtering as erosion mechanism. The chemical erosion is calculated using the weight loss measurement data published in [10,11]. Clearly, physical sputtering alone is not sufficient to explain the degree of erosion of the graphite probes. The addition of chemical sputtering, however, makes the agreement between data and calculation quite reasonable and certainly within the error bars of the experiment.

Figs. 5 and 6 show the toroidal and poloidal distribution of W and Cu erosion for the successive campaign. Again, the measurement is compared with the calculation. Apart from the excellent agreement, it is interesting to note that the Cu erosion is ~30 times larger than for W and also that while Cu presents an asymmetric profile, W does not (see also Fig. 3). In Fig. 5, in sectors 2, 3, 12 an 13, the Cu erosion is much higher than everywhere else, the same applies for the upper and lower divertor positions (2 and 8) of the poloidal profile (Fig. 6). In both cases, the higher erosion

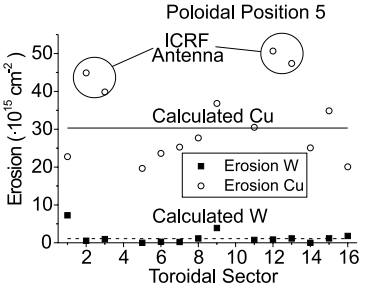

Fig. 5. Toroidal distribution of W and Cu erosion during the campaign following the one in which the W coated test tiles were exposed (November 1999–February 2000). In the graph, the expected erosion from sputtering by CX neutrals is plotted for comparison of both Cu and W. The higher Cu erosion in sectors 2, 3, 12 and 13 corresponds to the position of the RF antenna.

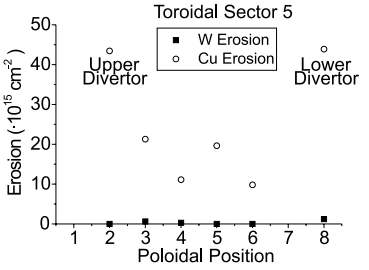

Fig. 6. Poloidal distribution of W and Cu erosion during the campaign following the one in which the W coated tiles were exposed (November 1999–February 2000). The higher Cu erosion in poloidal positions 2 and 8 corresponds to the position of the upper and lower divertors, respectively.

can be explained by the higher particles recycling in proximity of the RF antenna, between sectors 2 and 3 and 12 and 13, and of the divertors. This effect is not seen in the W probes because these recycling particles have usually a quite low energy (<100 eV) and are therefore below the quite high W sputtering threshold of ~210 eV for D. The B2/EIRENE simulation at low (3.2×10^{19} m^{-3}) and high (5.2×10^{19} m^{-3}) density used in the modified version of the sputtering code (to take into account the different energy distribution and sputtering yield of a deuterium plasma) appears to reproduce the data quite well.

As these simulations have been successfully tested for low (C), medium (Cu) and high (W) Z materials, one can infer that the simulations for other fusion relevant materials are similarly representative of the real erosion for the selected material. Therefore, simulations have been also done for Be, Al, stainless steel and Mo erosion rates, and a figure of merit (F. of M.) for the various materials at low and high plasma density has been calculated. The F. of M. of the different materials is defined as the normalisation of the ratio between the maximum allowed concentration of the material in the plasma and the material erosion rate. The maximum allowed concentrations of the various materials in a ~10 keV plasma are taken from [5]. The so defined F. of M. does not include any information on the penetration probability, which is known to be material dependent but it is not known for all the materials in question. A high value of the F. of M. indicates of course a more favourable material. Figs. 7(a) and (b) show the F. of M. for the above mentioned materials and a low and high density deuterium plasma, respectively, for the inner and outer wall of ASDEX Upgrade. As can be seen, the medium Z materials are the least favourable and W is more favourable at high plasma density. Be, however, is always more favourable than W especially at low density and in the outer wall. C, if chemical sputtering is included, is comparable to W at high density but sensitively better at low plasma density.

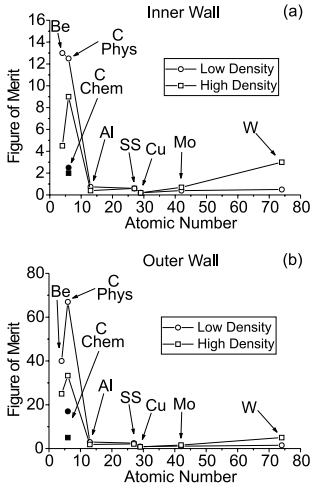

Fig. 7. F. of M. calculation for several first wall materials in both a high and low density plasma discharge for the inner (a) and outer (b) wall of ASDEX Upgrade. For C, the F. of M. is calculated both for physical sputtering only (open symbols) and for physical and chemical sputtering (solid symbols).

As a next step reactor is envisaged to operate with a D–T mixture, it is important to probe the plasma isotope dependence of the first wall candidate materials (Be, C and W). Figs. 8(a) and (b) plot the figures of merit for the three materials for the low and high density cases of the three plasma isotopes (H, D and T), for the inner and outer wall, respectively. As can be seen, the tungsten F. of M. suffers from a quite large isotope dependence, which is especially marked in the inner wall. Although

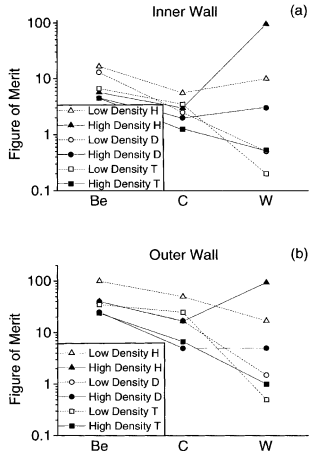

Fig. 8. Isotope dependence of the F. of M. calculation for Be, C and W at the inner (a) and outer (b) wall of ASDEX Upgrade for a high and low density plasma discharge. The open symbols indicate low density, the full ones high density. Triangles are used for a hydrogen plasma, circles for a deuterium one and squares for a tritium one.

Be and C figures of merit are also somewhat isotope dependent, the effect is not comparable in magnitude with the W one. For this reason, a W wall with H plasma is clearly better (in the inner) than Be wall (equivalent in the outer). This is in agreement with what was reported in [2], however, if one considers a D–T plasma, then Be F. of M. becomes between 4 and 10 times better than the W one for a high density discharge and ~35 times better for a low density plasma.

4. Conclusions

The measured erosion of the four W coated heat shield tiles is found to be comparable to calculations based on CX neutrals sputtering in the upstream half of the tiles. On the downstream side, however, with exception of the uppermost tile, the erosion is a factor of ~3 larger. This greater amount of erosion appears to be due to an additional ion sputtering component. As ion erosion can be excluded both in the divertor phase of all discharges and in the heated limiter phase of the ITB pulses, one can infer that the ion erosion is due to the initial limiter phase of all discharges. During the start-up phase, the low density plasma is sufficiently hot to justify W sputtering. If the measured W erosion is scaled to full W tile coverage of the heat shield, a total W release of $\sim 1.7 \times 10^{17}$ atoms/s is calculated. This implies a ratio W/D $\sim 10^{-6}$, assuming a penetration probability of 0.03 [12] and a particle residence time of ~0.1 s. This number is a factor of ~10 lower than the maximum W tolerable concentration. Furthermore, one must notice that this still represents an upper limit because the included ion erosion component could be avoided by starting the plasma on a specially suited non-W limiter.

The erosion profiles of the LTS toroidally and poloidally distributed around the outer wall show a W erosion much smaller than the one of the low (~200 times) and medium Z materials (~30 times). Moreover, the low and medium Z materials erosion mainly depends on n_i and is concentrated around the high recycling regions like RF antenna and divertors. Furthermore, the measured erosion for different materials and different campaigns agrees quite well with the calculated one.

As the calculated erosion has been successfully tested against experimental results, erosion rate calculations can be done and compared for different materials, for different plasma densities, fuel isotopes and for the inner and outer wall of the tokamak. From these calculations, a F. of M. among the different materials can be defined as the normalised ratio between the maximum allowed concentration of the given impurity in the plasma with its erosion rate. F. of M. calculations show that Be, C and W are better than medium Z materials like Fe, Mo and stainless steel. It is also clear that the W F. of M., in contrast to Be and C, is strongly isotope dependent. For this reason, if an appropriate D–T mixture plasma is considered, then the Be F. of M. appears to be clearly better than that of tungsten. The opposite is the case for a hydrogen plasma. Of course, when a material is selected for a next generation fusion device, not only the F. of M. has to be considered but also the actual values of the material erosion rate, which ultimately set the first wall lifetime. For a high density ASDEX Upgrade plasma, the Be erosion rate at the inner heat shield would be $\sim 4.5 \times 10^{18}$ atoms/m^2 s, while for W, the same would be $\sim 5.0 \times 10^{15}$ atoms/m^2 s, a factor of ~1000 smaller and therefore an equally longer first wall lifetime.

Acknowledgements

The authors are grateful to the following people who in various ways contributed to this paper: D. Coster, A. Kukushkin, R. Neu, V. Rohde, J. Stober.

References

[1] W. Eckstein, C. Garcia-Rosales, J. Roth, W. Ottenberger, IPP Report, IPP 9/82.
[2] H. Verbeek, J. Stober, D. Coster, W. Eckstein, R. Schneider, Nucl. Fus. 38 (1998) 12.
[3] Technical Basis for the ITER Final Design Report, Cost Review and Safety Analysis, (FDR) ITER EDA Documentation Series No. 16, IAEA, Vienna, 1998.
[4] H. Maier, K. Krieger, A. Tabasso, S. Lindig, V. Rohde, J. Roth, The ASDEX Upgrade Team, in: Proceedings of the 26th European Conference, vol. 23J, Maastricht, ECA, 1999, p. 1509.
[5] J. Wesson, Tokamaks, Oxford University, Oxford, 1987, p. 202.
[6] A. Tabasso, H. Maier, K. Krieger, J. Roth, ASDEX Upgrade Team, Nucl. Fus. 40 (2000) 1441.
[7] A. Tabasso, J. Roth, H. Maier, K. Krieger, The ASDEX Upgrade Team, in: Proceedings of the 26th European Conference, vol. 23J, Maastricht, ECA, 1999, p. 1533.
[8] A. Kukushkin, private communications.
[9] D. Coster, private communications.
[10] J. Roth, J. Nucl. Mater. 266 (1999) 51.
[11] M. Balden, J. Roth, J. Nucl. Mater. 279 (2000) 351.
[12] R. Neu, V. Rohde, D. Bolshukhin, A. Geier, A. Kallenbach, K. Krieger, H. Maier, R. Pugno, K. Schmidtmann, M. Zarrabian, ASDEX Upgrade Team, these Proceedings.